# Prediction of Water Seepage into a Geologic Repository for High-Level Radioactive Waste

Jens Birkholzer, Sumit Mukhophadhyay, Yvonne Tsang

*Ernest Orlando Lawrence Berkeley National Laboratory,*

*1 Cyclotron Road, MS 90-1116, Berkeley CA 94720*

*phone (510) 486-7134; fax (510) 486-5686*

*jtbirkholzer@lbl.gov*

Text pages (including list of tables and figures): 29

Number of tables: 1

Number of figures: 8

**Abstract**–*Predicting the amount of water that may seep into waste emplacement drifts is important for assessing the performance of the proposed geologic repository for high-level radioactive waste at Yucca Mountain, Nevada. The repository would be located in thick, partially saturated fractured tuff that will be heated to above-boiling temperatures as a result of heat generation from the decay of nuclear waste. Since infiltrating water will be subject to vigorous boiling for a significant time period, the superheated rock zone (i.e., rock temperature above the boiling point of water) can form an effective vaporization barrier that reduces the possibility of water arrival at emplacement drifts. In this paper, we analyze the behavior of episodic preferential flow events that penetrate the hot fractured rock, evaluate the impact of such flow behavior on the effectiveness of the vaporization barrier, and discuss the implications for the performance assessment of the repository. A semi-analytical solution is utilized to determine the complex flow processes in the hot rock environment. The solution is applied at several discrete times after emplacement, covering the time period of strongly elevated temperatures at Yucca Mountain.*

# 1. INTRODUCTION

Seepage refers to the flow of liquid water into underground openings. In geologic repositories for high-level radioactive waste, seepage defines the amount of water that can contact waste packages in the emplacement tunnels (drifts) and that may potentially promote the corrosion of waste canisters. In case of waste package failure, seepage also defines the mobilization rate of radionuclides. The more water enters the emplacement drifts, the more radionuclides can be picked up and transported into the surrounding rock. Therefore, predicting the amount of seepage into drifts is essential in assessing the performance of the proposed geologic repository for high-level radioactive waste at Yucca Mountain, Nevada.

The proposed repository site at Yucca Mountain is located in the unsaturated fractured rock zone about 300 m below the ground surface and about the same distance above the water table. The unsaturated rock layers overlying and hosting the repository form a natural barrier that can reduce the amount of infiltration water entering emplacement drifts. Two processes contribute to reducing seepage: The first is the result of capillary forces forming at the drift wall, which tend to divert water flow around the underground opening [1]. The second process is related to the heat generated by the radioactive waste, giving rise to above-boiling temperatures in the drift vicinity for several hundred years after waste emplacement. Consequently, water infiltrating down towards the repository is subject to vigorous

vaporization in the fractured rock, thereby reducing the possibility of water arrival at the drifts [2]. The present analysis addresses the issue of seepage at strongly elevated rock temperatures in the drift vicinity (hereafter referred to as thermal seepage) and estimates the effectiveness of the vaporization barrier formed by the superheated rock zone around drifts.

The thermal-hydrological conditions in the unsaturated fractured rock at Yucca Mountain following waste emplacement have been investigated in various modeling studies using sophisticated process models [e.g., 3, 4, 5, 6, 7, and 8]. Modeling results have demonstrated that boiling of rock water will give rise to significant thermal and hydrological perturbation of the ambient state. As the water in the vicinity of waste emplacement drifts vaporizes, a superheated dry rock region of up to 5 m in extent forms around the drifts. The vapor moves away from the drifts through the permeable fracture network, driven primarily by the pressure increase caused by boiling. In cooler regions away from the drift, the vapor condenses in the fractures, generating a region of elevated water saturations and downward fluxes. Simulation results indicate that these increased fluxes do not result in water arrival at the drifts during the above-boiling period, suggesting a fully effective vaporization barrier. However, this finding may be in part attributed to the spatial and temporal averaging employed in the above modeling studies (which are based on a continuum assumption), since the possibility of small-scale flow processes—such as formation of episodic preferential pathways

(finger flow)—is underestimated. Different results may be obtained from model concepts that explicitly consider small-scale episodic preferential flow events carrying water at flow rates much larger than the average flow. Such small-scale flow events may penetrate far into the superheated rock to eventually reach the emplacement drifts [9].

In this paper, the potential impact of episodic preferential flow events on thermal seepage is studied in a systematic manner. It is assumed that such flow events originate somewhere in the rock region of elevated saturation above the drifts (condensation zone) and percolate downward towards the emplacement drifts. Figure 1a shows an illustration of episodic fingers flowing through fractures and penetrating into the superheated rock above waste emplacement drifts. As flow arrives at the superheated rock region around drifts, water begins to boil off. Depending on the magnitude and duration of each flow event, and the temperature and pressure conditions in the superheated rock, water may completely vaporize above the drift crown, or it may penetrate far into the superheated region and eventually reach the drift. In our study, a semi-analytical solution [10] is used to simulate the complex flow processes of episodic finger flow under thermal conditions. With this solution, the maximum penetration distance into the superheated rock is determined for specific episodic flow events and thermal conditions, and the amount of water arriving at the drift crown is calculated.

## 2. CONCEPTUAL MODEL

The first step in our analysis is to derive estimates of the potential characteristics of episodic finger flow at Yucca Mountain. Experimental data from a comprehensive laboratory study [11] are used for this purpose, and a simplified finger-flow model for downward drainage is developed (Section 2.1). The second step is to simulate the fate of such episodic finger-flow events when the flow penetrates into the superheated rock region above waste emplacement drifts, using the semi-analytical solution developed in [10]. This solution is briefly described in Section 2.2. The solution is implemented at several discrete times after waste emplacement to cover the expected range of rock temperature conditions and the extent of the superheated zone around drifts. These selected times and the respective rock temperature conditions are described in Section 2.3.

The third step is to evaluate the results, namely the potential for water arrival at the drift at different times after emplacement. The amount of water arriving at the drift crown is evaluated in relation to the perturbed flow situation above the drifts, i.e., in relation to the elevated downward flux from the condensation zone towards the drift, as simulated from the above mentioned process models using continuum assumptions. Note that water arrival at the drift does not necessarily mean that this water will actually seep into the drift, since the open cavity acts as a capillary barrier, diverting

downward flow around the tunnel. This additional barrier caused by capillarity is not considered in the episodic finger-flow model.

### 2.1. Characteristics of Episodic Preferential Flow

Episodic preferential flow in unsaturated fractures has been experimentally observed in flow visualization experiments using fracture replicas (e.g., 11, 12, and 13). Although constant and uniform inlet flow conditions were applied in these experiments, intermittent flow behavior was caused by small-scale capillary barriers within the fracture plane, forming in areas of smaller apertures located above regions of larger apertures. As a result, water accumulated in the small-aperture regions until the water potential exceeded the capillary-force difference. Once this occurred, a large portion of the accumulated water moved rapidly downward in a thin finger. When the capillary pool emptied, the finger snapped and reformed at some later time. Typically, the observed water volumes per event were small, on the order of milliliters.

In our study, we assume that such intermittent flow behavior can also occur in the unsaturated fractures at Yucca Mountain, particularly during the thermal period when condensate above the superheated zone is expected to provide a significant source of water above waste emplacement drifts. Since there are neither experimental studies with fracture test samples from Yucca Mountain nor replicas mimicking Yucca Mountain fractures, we use the flow characteristics observed in the above experiments as estimates for potential

episodic preferential flow in unsaturated fractures at Yucca Mountain. Of the experimental studies cited above, the fracture replica analysis in [11] is probably best suited for this purpose, because the realistic geometry of natural fractures is accounted for, and detailed quantitative measurements are provided in their analysis. The fracture replica in this experimental work was taken from the granitic rock of the Stripa Mine in Sweden. Differences between fractures from the Yucca Mountain tuff and the Stripa Mine granite—with respect to aperture distributions, surface roughness, and contact angle—will bring out differences in flow behavior and distribution. This approach is valid for a qualitative analysis intended to demonstrate the impact of an alternative flow concept on water arrival at the drift during the thermal period at Yucca Mountain.

The range of water volumes accumulating in and draining from capillary pools as reported in [11] is small over the entire suite of experiments, and largely unaffected by the order-of-magnitude variation in flow rate imposed at the inlet boundary. Also, the width of the rivulets was observed to be independent of the applied flow rate, whereas the temporal frequency of flow events correlated well with the flow rate at the inlet boundary condition. These observations are consistent with the concept of geometry-induced episodic flow patterns, in which the accumulation and flow distribution of water depends on local aperture variation, while the time between subsequent flow events—required for water accumulation—depends on the rate of overall

downward infiltration in the fractured rock. Adopting this concept for the thermal conditions at Yucca Mountain, the characteristics of individual fingers draining down from the condensation zone (i.e., finger geometry, water volume per flow event and flow rate) are assumed to be independent of the average downward flux. Their frequency, however, is directly correlated to the average downward flux; i.e., strongly elevated downward fluxes at early stages of heating result in finger flow that occurs more often in time and space.

Basic characteristics defining episodic finger flow, namely water volume of individual flow events V, fracture aperture b, and finger width w, are directly extracted from the experimental results described in [11]. Using representative values for these parameters, additional parameters are derived from a simplified conceptual flow model, assuming gravity-driven, laminar, and fully developed flow in vertical one-dimensional rivulets of uniform width, in fractures of uniform aperture and infinite extent. These derived parameters—flow velocity $v_P$, mass flow rate $m_P$, and duration of flow $t_P$—are input required for the semi-analytical solution described in Section 2.2. Following the above assumptions, the downward flow velocity of the finger, $v_P$, can be calculated from:

$$v_P = \frac{b^2}{12}\frac{\rho g}{\mu} \qquad \text{(Eq. 1)}$$

where ρ is density of water, g is gravitational acceleration, and μ is the dynamic viscosity of water. The mass flow rate, $m_P$, of the finger flow can be calculated as follows

$$m_P = \rho b w v_P , \qquad \text{(Eq. 2)}$$

and the duration of the finger flow, $t_P$, is given from mass continuity

$$t_P = \frac{\rho V}{m_P} \qquad \text{(Eq. 3)}$$

The flow duration denotes the time period needed for the finger to flow past a given location.

Table 1 lists the values extracted from [11] and the calculated flow characteristics of all simulation cases. The so-called Base Case uses the geometric mean values of fracture aperture and water volume given in [11]. For finger geometry, a fairly consistent finger width of about 1 mm is reported in [11], often forming behind advancing water drops that are slightly larger, on the order of 4.5 mm. Since these two values are not sufficient to derive statistical properties, we use the more conservative case with $w = 1$ mm. (Assumptions that potentially lead to a higher amount of water arrival at the drift are considered "conservative" in this paper.) The other cases are sensitivity cases, adjusting the Base Case value of either fracture aperture or water volume by adding/subtracting the respective standard deviation values (in log space), also extracted from [11]. With the water volume and the finger

width kept constant, changes in fracture aperture invoke changes in flow velocity, mass flow rate, and flow duration (Cases A and B). A large aperture is associated with a fast, intense, and short flow event. Changes in water volume, while keeping aperture and width constant, affect only the flow duration (Cases C and D). A large volume is related to a long flow duration.

## 2.2 Water Penetration into Superheated Rock

The semi-analytical solution described in [10] is used to determine the maximum penetration distance of episodic fingers subject to vaporization from the hot rock. In case the finger penetrates through the entire superheated zone above the drift, the solution also gives the total amount of water arriving at the drift crown. A brief review of the mathematical formulation and solution procedure is given below. Note that this solution is an extension of the analytical solution presented in [14]. However, [14] describes an approximate asymptotic solution for long-term behavior of continuous finger flow, while the semi-analytical solution in [10] provides an exact simulation method for early and late time periods of flow events that can be episodic or continuous.

The basic conceptual model for the semi-analytical solution of finger penetration into superheated rock is schematically depicted in Figure 1b, showing a superheated region of length $L$ above the crown of a waste emplacement drift. Here, the ambient rock water has been boiled off, and

fractures and rock matrix are essentially dry. The rock temperature in the superheated zone is above the boiling temperature at prevailing pressure. Initially, before finger flow occurs, the temperature field is uniform in the lateral $x$-direction and a function of location in the vertical $z$-direction. Episodic flow events of a given mass flow rate $m_P$, duration $t_P$, and finger width $w$ enter the superheated region at $z = 0$ and $t = 0$. The percolating water is already heated to almost boiling temperature $T_P$ upon arrival at the superheated region and begins boiling as it passes the boiling-point isotherm. As presented in the previous section, the downward flow of the finger is gravity-driven and strictly one-dimensional.

Upon contact with the water, the rock surface cools to boiling temperature, and a steep temperature gradient is established in the surrounding matrix when the liquid front in the fractures reaches the considered position. With time, the thermal perturbation penetrates further into the rock, the thermal gradient decreases, and heat flow from the matrix to the fracture is reduced. Because conduction in the matrix is slow compared to the vertical movement of the liquid pulse, the conductive heat flow within the matrix and from the matrix to the fracture is considered to be strictly lateral, perpendicular to the fracture plane. Note that the period between two consecutive episodic flow events is longer than the flow duration $t_p$, so that for all practical purposes the rock temperature, perturbed from contact with one flow event, has equilibrated to its initial state before the next flow event arrives.

The downward flow rate at location $z$ in the superheated region can be derived from an energy balance between the energy required for vaporization of water and the energy supplied by heat conduction from the rock. This energy balance is given in [10] as follows

$$\frac{\partial m(z,t)}{\partial z} = -\frac{2wk_m}{h}\frac{T_{RI}-T_P}{\sqrt{\pi\kappa\left(t-t_0(z)\right)}} \qquad \text{(Eq. 4)}$$

using an analytical solution given in [15] for the lateral temperature distribution in the rock matrix. Here, $m$(z,t) is mass flow rate at location $z$ and time $t$, $k_m$ is rock thermal conductivity, $h$ is specific enthalpy of vaporization, $T_{RI}$ is the initial rock temperature, and $\kappa$ is rock thermal diffusivity. The period $t_0(z)$ denotes the time interval after initial entry of the water finger into the superheated zone until the arrival of the tip of the liquid finger at location $z$. Equation (4) is valid as long as the thermal perturbation in the rock is nearly uniform across the width of the liquid finger. Since thermal perturbation grows with $(\kappa t)^{1/2}$, the maximum time period $t_m$ associated with uniform thermal perturbation is on the order of

$$t_m = \frac{w^2}{\kappa} \qquad \text{(Eq. 5)}$$

For $t > t_m$, the nearly one-dimensional heat flow perpendicular to the fracture-rock interface transforms to a more cylindrical spreading of heat.

A simple Lagrangian solution scheme was presented in [10] that solves Equation (4) for episodic flow events of a given flow rate and duration. A

time-marching procedure tracks the movement of finite water masses traveling downwards while part of the water boils off. The semi-analytical solution scheme was shown to be accurate, robust, and fast. For details on the numerical methods, we refer the reader to [10].

### 2.3 Predicted Thermal Conditions at Yucca Mountain

The long-term evolution of thermal-hydrological conditions in the rock is accounted for by applying the semi-analytical solution at 11 selected times after waste emplacement, covering the time period during which repository temperatures remain above boiling (about 1,000 years). The thermal parameters required as input for the semi-analytical solution, namely the vertical temperature profile and the extent of the superheated region, are obtained from drift-scale thermal-hydrological numerical simulations using a multiphase process model, based on a continuum assumption simulating the average flow behavior in the fractured rock [8].

Figure 2 shows results from this model for a representative waste emplacement drift, assuming an initial heat load of 1.45 kW/m (line load measured along drift length) at the time of emplacement. According to the current repository design, this heat load represents the average heat output of all waste packages at the time of emplacement. The initial value of 1.45 kW/m decreases with time as a result of radioactive decay. The peak temperature of the rock close to the drift is about 128$^{o}$C at 75 years after emplacement. The

superheated zone is largest between 100 and 450 years of heating, with a maximum extent of 4.19 m above the drift crown. The model simulations indicate that the temperature profile in the superheated region can be approximated by a linear distribution between the maximum temperature at the drift wall and the boiling temperature (i.e., 96 $^{o}$C) at the top of the superheated rock region. Using this approximation, the rock temperature at each vertical location in the superheated zone is defined. Note that we apply the same multiphase process model described in [8] to derive estimates for the thermally induced flow perturbation in the condensation zone above the repository (see Figures 6, 7, and 8).

# 3. RESULTS

## 3.1. Base Case Analysis

To gain a basic understanding of the mechanisms of episodic preferential flow events in hot fractures around drifts, we first focus on the Base Case flow event. The semi-analytical solution in [10] is employed to evaluate the effect of vaporization once the water has entered the superheated rock zone. The thermal properties of the rock matrix are based on measured values from the repository rock units at Yucca Mountain. For illustration of results, we choose one time snapshot at 550 years after emplacement. According to Figure 2, the vertical extent of the superheated rock at this time is 3.54 m, with a maximum rock temperature at the drift wall of 105.8$^{o}$C. Thus, the episodic flow event entering this zone encounters a temperature field of 96$^{o}$C at a location of 3.54 m above the drift crown, which is assumed to increase linearly to 105.8$^{o}$C at the drift wall.

Figure 3 shows the penetration of the tip of the draining finger versus time, with $z = 0$ the top of the superheated domain and $t = 0$ the time when the tip of the finger enters the boiling zone. (The arrow gives the penetration curve for water flowing with undisturbed velocity $v_P$ = 0.054 m/s.) Clearly, after about 2 m, the penetration of the finger slows down noticeably compared to $v_P$. The farther the finger infiltrates, the stronger this effect is, an effect caused by boiling of water. For illustration purposes, we may use the semi-analytical solution to calculate the maximum penetration of the finger in the

absence of the drift opening; i.e., we assume that the superheated fractured rock zone extends farther down while the thermal gradient remains the same. In this case, the episodic flow event would end after about 4.17 m, when all water has vaporized. (Note that the time period of finger flow in these cases is longer than the time period $t_m$ according to Equation (5) in which uniform thermal perturbation across the width of the finger can be safely assumed. Applying the semi-analytical solution for times larger than $t_m$ does not account for the more cylindrical spreading of heat in the rock, and therefore underestimates the amount of thermal energy available for boiling of water, leading to conservative estimates of the amount of water arriving at the drift crown.)

After investigating whether episodic preferential flow can overcome the vaporization barrier to arrive at the drift crown, we will now focus our attention on the amount of water reaching the drift. Obviously, the water mass flowing past a given location in the superheated rock decreases with penetration distance, owing to vaporization as the liquid pulse moves down the fracture. The farther the infiltrating finger penetrates into the superheated region, the less water is available. This is demonstrated in Figure 4, where the total amount of water breakthrough is plotted as a function of vertical penetration distance, given relative to the initial water volume entering the superheated rock. While the major fraction of the initial water volume vaporizes in the superheated rock, still about 16.5% of it arrives at the drift crown.

The above results indicate that the relative rate of water arriving at the drift crown is small at 550 years. However, this relative rate needs to be evaluated in conjunction with the flux perturbation in the condensation zone above the repository. Water accumulation in this zone increases the average downward flux towards the superheated zone. Thus, following the conceptual model outlined in Section 2.1, episodic flow events could more frequently—in time and space—originate from the condensation zone, thereby increasing the absolute amount of water arriving at the drift. (It is assumed that the characteristics of individual fingers are not affected by the change in average downward flux). According to results from [8], the maximum downward flux in the fracture continuum above the drift is about 28 mm/yr at 550 years, which is about 4.6 times higher than the natural infiltration of about 6 mm/yr at Yucca Mountain. We may conservatively assume that this elevated flux drains down entirely in an episodic, finger-type manner. Then the potential water arrival at the drift crown—including the combined effect of flux elevation and vaporization barrier—can be estimated by multiplying the thermally elevated flux of 28 mm/yr by the relative rate of mass arrival at the drift (from the semi-analytical solution). At 550 years, with 16.5% of the initial water volume arriving at the drift, the resulting flux at the drift crown would be 4.6 mm/yr. Thus, the thermally enhanced downward flux in the condensation zone is effectively reduced by vaporization to a flux rate that is smaller than the natural infiltration rate. While exclusion of water from

penetrating down to the drifts may not be absolute at the considered time, the vigorous boiling in the superheated rock still acts as a valuable barrier.

The above analysis, conducted for conditions at 550 years, can be performed for the selected 11 time steps that cover the time period during which rock temperature is above boiling (see Section 2.3). Figure 5 provides results of the semi-analytical solution considering these 11 discrete time steps. The diamond symbols give the maximum penetration distance into the superheated rock, while the circular symbols show the relative amount of water arriving at the drift. The maximum penetration distance should be compared to the dotted curve showing the extent of the superheated region above the drift crown. According to this figure, no water would reach the drift for the first 450 years after emplacement, caused by intense heat and a sufficiently large superheated region. At later times, the possible maximum penetration (in the absence of the drift opening) becomes larger than the boiling zone extent; i.e., water would arrive at the drift crown. The relative amount of water reaching the drift increases significantly between 450 years and 750 years after emplacement, as a result of the decreasing rock temperature and the shrinking superheated rock zone. Eventually, after 950 years, the effect of vaporization becomes marginal, so that the water mass arriving at the drift is almost equal to the initial mass.

In Figure 6, the calculated relative rates of water arriving at the drift crown at the given times are related to the average flux perturbation in the condensation zone at those times. The dashed line shows the so-called flux-elevation factor, defined as the maximum downward flux in the condensation zone, divided by the natural infiltration rate. As the circular symbols indicate, the most significant flux elevation occurs at 75 years of heating, where the maximum downward flux is 73.2 mm/yr, more than 12 times that of the ambient flux of 6 mm/yr. Over time, this effect declines rapidly and is essentially negligible at 1,500 years after waste emplacement. (The spike at 650 years is caused by an assumed change in climate at 600 years, leading to an increase in natural infiltration at Yucca Mountain.) The solid line gives the water flux arriving at the drift crown when the combined effect of flux perturbation and vaporization barrier is considered. Note that this flux is given relative to the natural infiltration rate at the respective time and is obtained by multiplying the flux-elevation factor by the relative water-arrival rate given in Figure 5. If the displayed values are larger than one, the amount of water potentially arriving at the drift wall exceeds the natural infiltration rate.

As is clear from Figure 6, vaporization reduces the impact of flux perturbation in the condensation zone by a large percentage. For the first 450 years of heating, vaporization is so effective that the amount of water potentially arriving at the drift crown is zero. Between 450 and 650 years, vaporization is still strong enough to reduce the elevated fluxes to values

smaller than the natural infiltration rate (i.e., the resulting flux ratio is smaller than one). This clearly demonstrates that the period of strongly elevated vertical flux in the condensation zone coincides with the period of very effective vaporization. Thus, even if the downward flux from the condensation zone towards the drift would flow entirely in episodic finger-type patterns—an extreme flow conceptualization that has never been observed at Yucca Mountain—the vaporization barrier would be fully effective for several hundred years. Only at later times, when vaporization effects diminish, is the flux arriving at the drift slightly higher than the natural infiltration rate. However, seepage of water into the drift should not be expected from this limited water arrival, because such small flow rates will be effectively diverted around the drift by the capillary barrier capability of the open cavity [1]. Also note that these results are based on many conservative assumptions with respect to the amount of water reaching drifts, most of them related to the idealized conceptual model of finger flow and heat transport.

### 3.2 Sensitivity Cases

Several sensitivity cases are studied to analyze the uncertainty of water arrival at the drift caused by variability in the flow characteristics of episodic finger flow. Of all input parameters required for the semi-analytical solution, those properties related to the small-scale finger-flow characteristics, as extracted from [11], are probably the most uncertain and variable. In contrast, thermal properties of the rock and the future thermal conditions at Yucca

Mountain are well constrained by laboratory data, *in situ* measurements, and associated modeling work. Thus, in the sensitivity study, we vary fracture aperture and initial water volume per flow event, causing changes in the finger flow properties $v_P$, $m_P$, and $t_P$ as given in Table 1. The finger width, the thermal properties of the rock, and the temperature conditions remain unchanged. Results of the sensitivity analysis are given in Figure 7 for Cases A and B (variation of fracture aperture) and Figure 8 for Cases C and D (variation of water volume). The heavy solid and dashed-dotted lines mark the potential water flux at the drift crown—under thermal conditions considering flux elevation and vaporization effects—relative to the natural infiltration rate for cases of large and small aperture (water volume), respectively. For comparison, the thin dotted line shows the respective Base Case results already given in Figure 6.

Fracture aperture is clearly a more sensitive parameter than water volume. For both parameters, a change to larger values gives rise to an increased potential for water arrival at the drift. Of all sensitivity cases, Case A (large fracture aperture) is the most critical. In this case, the episodic flow event is comparably fast and intense (large velocity and mass flow rate), and the boiling rate of water is limited by the reduced contact time between water and hot rock (small flow duration). However, even then, vaporization in the superheated zone is strong enough to significantly reduce the effect of elevated vertical fluxes draining down from the condensation zone,

particularly at early times when the thermal perturbation is largest. The maximum flux elevation ratio at the drift crown is about three at 550 years after emplacement; i.e., the amount of water potentially arriving at the drift would be 18 mm/yr, compared to 6 mm/yr at ambient. This is a relatively small increase that is not expected to result in seepage because the capillary barrier capability at the drift wall should effectively divert the water around the drift [1].

# 4. CONCLUSION AND DISCUSSION

Our study analyzes the fate of episodic finger flow penetrating into the superheated rock above waste emplacement drifts at Yucca Mountain during the time period of strongly elevated temperatures. A semi-analytical solution is utilized to calculate the maximum penetration depth into the superheated rock and, in case the finger flow penetrates down to the drift, to derive the amount of water arriving at the drift wall. The conceptual model is conservative with respect to the potential for water arrival, since the assumed finger-flow events are fast and intense compared to the average flux conditions at Yucca Mountain, and since vaporization effects are limited as a result of the small cross-sectional area between the penetrating water and the hot rock.

In spite of this conservatism, results of our study demonstrate that finger flow is not able to penetrate through the superheated rock during the first several hundred years of heating, when rock temperature is high and boiling conditions exist in a sufficiently large region above the drifts. These are the conditions in which the largest thermal perturbation occurs, or, in other words, when the potential for episodic finger flow is highest. Only later, when the superheated zone is small and the impact of vaporization is limited, can water arrive at the drift crown. However, the strong thermal perturbation observed at early heating stages has already diminished during this time period, and the net result of water arrival at the drift—considering the combined impact of

water buildup in the condensation zone and vaporization in the superheated zone—is similar to the natural infiltration rate. Seepage of water into the drift is not expected from this limited water arrival, because the flow should be effectively diverted around the drift by the capillary barrier capability of the open cavity [1].

The results of this study—i.e., most likely no seepage during the period of above-boiling temperatures—can have important performance implications for the proposed high-level radioactive waste at Yucca Mountain. For example, early canister failure as a result of localized corrosion during the time period of above-boiling drift temperatures can only occur in the presence of liquid water. Furthermore, if there were an early failure of the engineered barrier system, the release of radionuclides from the drifts into the rock would be strongly retarded in the absence of flowing water, because diffusive transport processes are extremely slow. In contrast, contaminant release into the natural environment would be much faster when water could seep into the drifts, pick up radionuclides and then drain down through the invert into the fractured rock. Thus, the vaporization and capillary barrier capabilities of the unsaturated rock in the vicinity of emplacement drifts would provide an effective safety mechanism for the repository.

It is important to realize that the conceptual model in our study includes a number of limiting assumptions that are valid for a qualitative evaluation, but

may not be interpreted as a quantitative representation of system behavior at Yucca Mountain. The most important limitation is that experimental data from a Stripa granite fracture are assumed to represent the characteristics of potential episodic finger flow in fractured tuff at Yucca Mountain. While this is a reasonable starting point for demonstration purposes, future experimental work on fractures of Yucca Mountain tuff would be beneficial to increase confidence about the validity of the underlying assumptions. Other assumptions, mostly conservative with respect to the simulated penetration distance, are related to the idealized conceptual model of finger flow and heat transport in the superheated rock. In spite of these limitations, our study has elucidated critical parameters and processes that are important in understanding water penetration of finger flow events into superheated fractured rock. This study has also helped to identify uncertainties inherent in these parameters and processes.

## REFERENCES


[1] Birkholzer, J.T., G. Li, C.-F. Tsang, and Y.W. Tsang, Modeling Studies and Analysis of Seepage into Drifts at Yucca Mountain, J. Contam. Hydrol., 38 (1-3), 349-384, 1999.

[2] Ramspott, L.D., The constructive use of heat in an unsaturated tuff repository, in Proceedings of the 2nd Annual High-Level Radioactive Waste Management Conference, Las Vegas, NV, 1991.

[3] Pruess, K., J.S.Y. Wang, and Y.W. Tsang, On thermohydrologic conditions near high-level nuclear wastes emplaced in partially saturated fractured tuff, 1, Simulation studies with explicit consideration of fracture effects, Water Resour. Res., 26, 1235-1248, 1990.

[4] Pruess, K., J.S.Y. Wang, and Y.W. Tsang, On thermohydrologic conditions near high-level nuclear wastes emplaced in partially saturated fractured tuff, 2, Effective continuum approximations, Water Resour. Res., 26, 1249-1261, 1990.

[5] Pruess, K., and Y.W. Tsang, Thermal modeling for a potential high-level nuclear waste repository at Yucca Mountain, Nevada, Rep. LBL-33597 UC-200, Lawrence Berkeley Lab., Berkeley, CA, 1993.

[6] Haukwa, C.B., Y.-S. Wu, and G.S. Bodvarsson, Thermal loading studies using the Yucca Mountain unsaturated zone model, J. Contam. Hydrol., 38 (1-3), 217-255, 1999.

[7] Buscheck, T.A, N.D. Rosenberg, J. Gansemer, and Y. Sun, Thermohydrologic behavior at an underground nuclear waste repository, Water Resour. Res., 38(3), 10-1 to 10-19, 2002.

[8] Birkholzer, J.T., S. Mukhophadhyay, and Y.W. Tsang, Modeling Water Seepage into Heated Waste Emplacement Drifts at Yucca Mountain, Proceedings TOUGH Symposium 2003, May 2003, Berkeley, CA, 2003.

[9] Pruess, K., and Y.W. Tsang, Modeling of strongly heat-driven flow processes at a potential high-level nuclear waste repository at Yucca Mountain, Nevada, Rep. LBL-35381 UC-600, Lawrence Berkeley Lab., Berkeley, CA, 1994.

[10] Birkholzer, J.T., Penetration of liquid fingers into superheated fractured rock, Water Resour. Res., 39(4), 9-1 through 9-21, 2003.

[11] Su, G.W., J.T. Geller, K. Pruess, and F. Wen, Experimental studies of water seepage and intermittent flow in unsaturated, rough-walled fractures, Water Resour. Res., 35(4), 1019-1037, 1999.

[12] Nicholl M. J., R.J. Glass, and S.W. Wheatcraft, Gravity-driven infiltration instability in initially dry nonhorizontal fractures, Water Resour. Res., 30(9), 2533-2546, 1994.

[13] Persoff, P. and K. Pruess, Two-phase flow visualization and relative permeability measurement in natural rough-walled rock fractures, Water Resour. Res., 31(5), 1175-1186, 1995.

[14] Phillips, O.M., Infiltration of a liquid finger down a fracture into superheated rock, Water Resour. Res., 32(6), 1665-1670, 1996.

[15] Carslaw, H.S., and J.C. Jaeger, Conduction of heat in solids, 2nd ed, Oxford University Press, Oxford, 1959.

## ACKNOWLEDGMENTS

This work was supported by the Director, Office of Civilian Radioactive Waste Management, U.S. Department of Energy, through Memorandum Purchase Order EA9013MC5X between Bechtel SAIC Company, LLC and the Ernest Orlando Lawrence Berkeley National Laboratory (Berkeley Lab). The support is provided to Berkeley Lab through the U.S. Department of Energy Contract No. DE-AC03-76SF00098. Review and thoughtful comments of Stefan Finsterle and Dan Hawkes from Berkeley Lab are gratefully appreciated.

## Table Captions

Table 1 Suite of episodic flow events flowing towards the superheated rock region

## Figure Captions

Figure 1. a. Schematic illustration of episodic finger flow in the unsaturated fractured rock surrounding heat-generating nuclear waste packages in emplacement drifts.

b. Conceptual model for finger flow in a vertical fracture above a drift with heat conduction from the adjacent rock.

Figure 2. Predicted temperature history at drift wall and extent of superheated rock above drifts

Figure 3. Maximum penetration of finger tip vs. time at 550 years of heating

Figure 4. Total water mass breakthrough at location z at 550 years of heating

Figure 5. Maximum penetration and percentage of water mass arriving at drift crown, at 11 different time steps after waste emplacement

Figure 6. Ratio of thermally perturbed vertical flux and natural infiltration.

Figure 7. Ratio of thermally perturbed vertical flux and natrual infiltration, showing sensitivity of model results to fracture aperture

Figure 8. Ratio of thermally perturbed vertical flux and natural infiltration, showing sensitivity of model results to initial water volume

# Tables

Table 1 Suite of episodic flow events flowing towards the superheated rock region

| **Simulation Cases** | **Fracture Aperture $b$ (mm)** | **Water Volume $V$ (mL)** | **Finger Width $w$ (mm)** | **Flow Velocity $v_P$ (m/s)** | **Mass Flow Rate $m_P$ (kg/s)** | **Flow Duration $t_P$ (s)** |
|---|---|---|---|---|---|---|
| Base Case | 0.141 | 0.161 | 1.0 | 0.054 | $7.3 \times 10^{-6}$ | 21.2 |
| Case A (large aperture) | 0.247 | 0.155 | 1.0 | 0.164 | $3.9 \times 10^{-5}$ | 4.0 |
| Case B (small aperture) | 0.081 | 0.155 | 1.0 | 0.018 | $1.4 \times 10^{-6}$ | 113.4 |
| Case C (large volume) | 0.141 | 0.249 | 1.0 | 0.054 | $7.3 \times 10^{-6}$ | 32.9 |
| Case D (small volume) | 0.141 | 0.104 | 1.0 | 0.054 | $7.3 \times 10^{-6}$ | 13.7 |
| | *Extracted from Su et al. (1999)* | | | *Derived using b, V, and w as input* | | |

# Figures

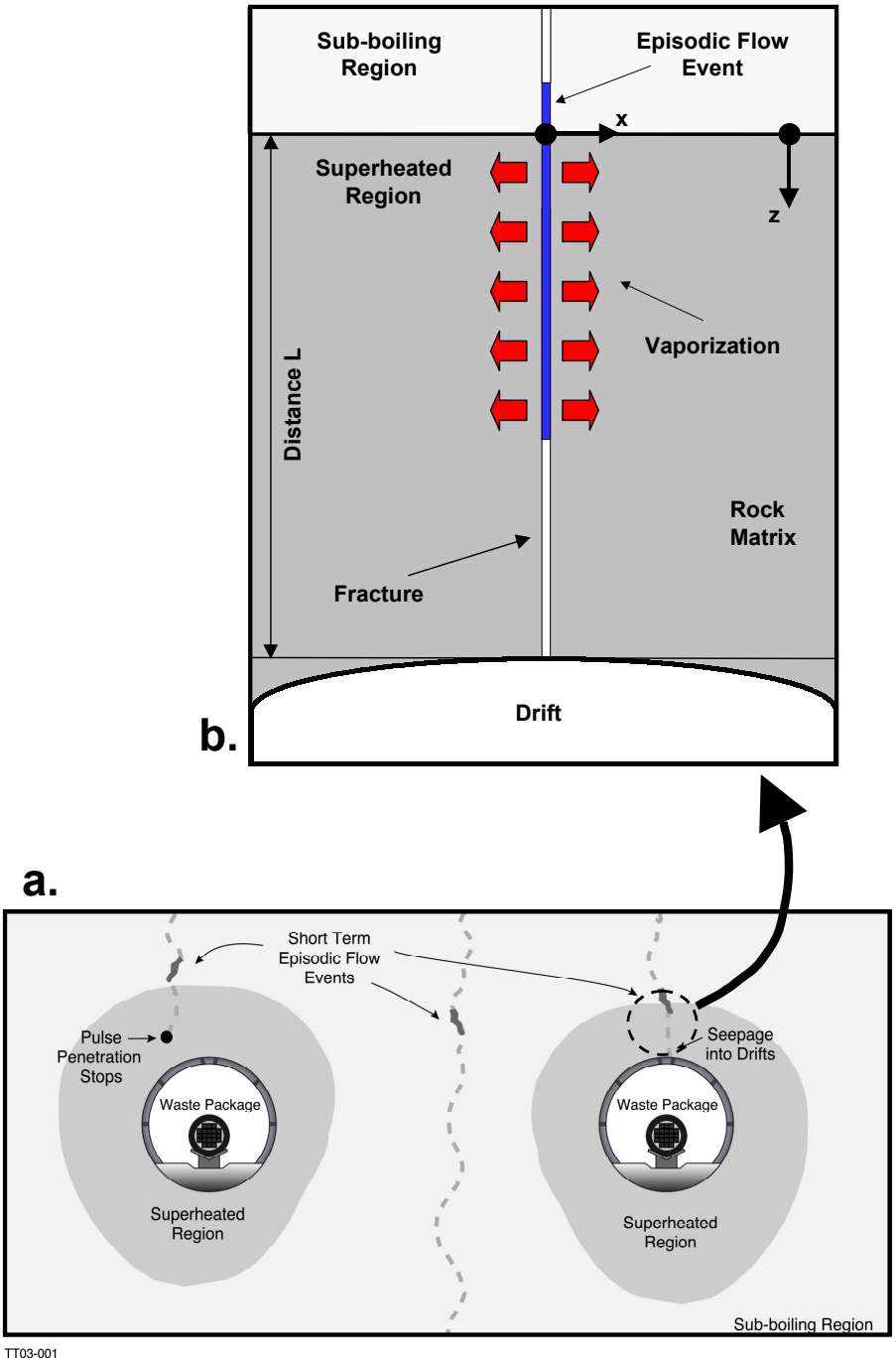


Figure 1. a. Schematic illustration of episodic finger flow in the unsaturated fractured rock surrounding heat-generating nuclear waste packages in emplacement drifts.
b. Conceptual model for finger flow in a vertical fracture above a drift with heat conduction from the adjacent rock.

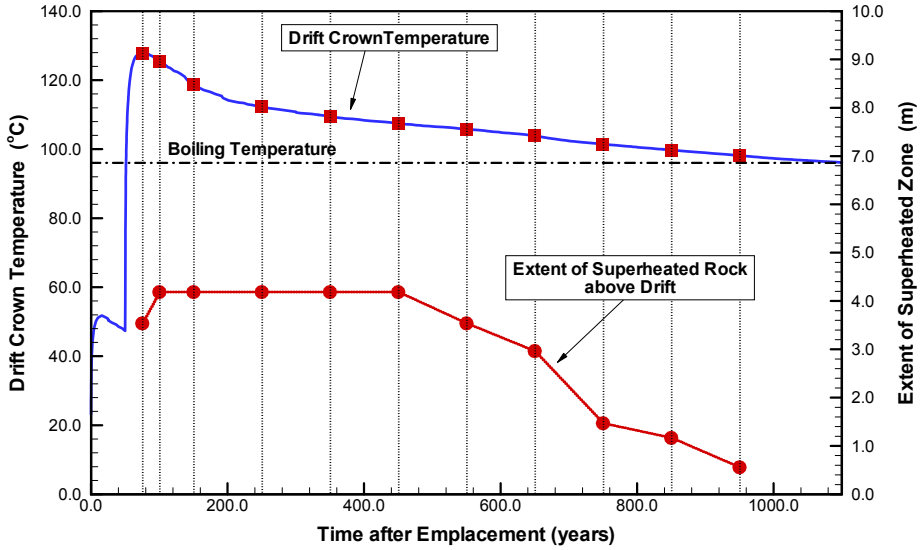


Figure 2. Predicted temperature history at drift wall and extent of superheated rock above drifts

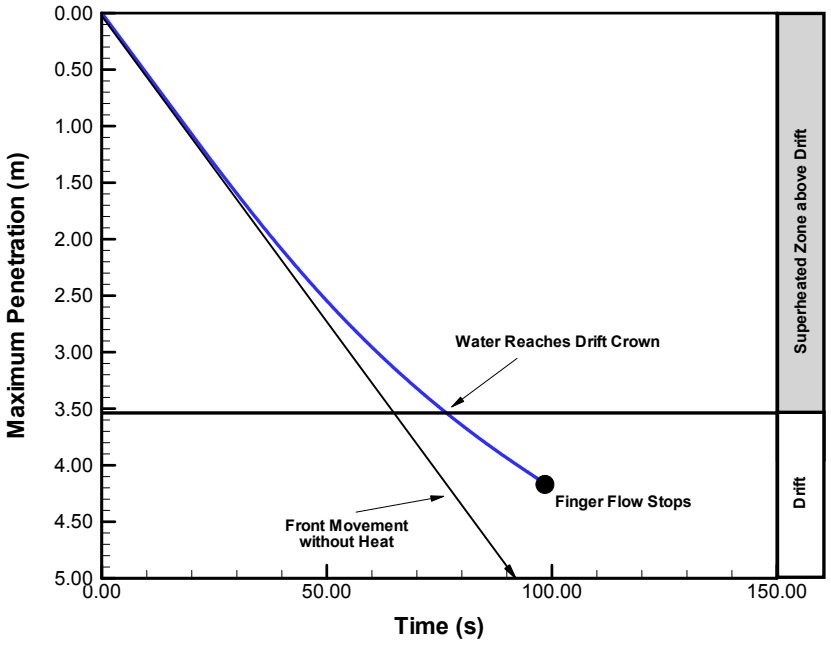


Figure 3. Maximum penetration of finger tip vs. time at 550 years of heating

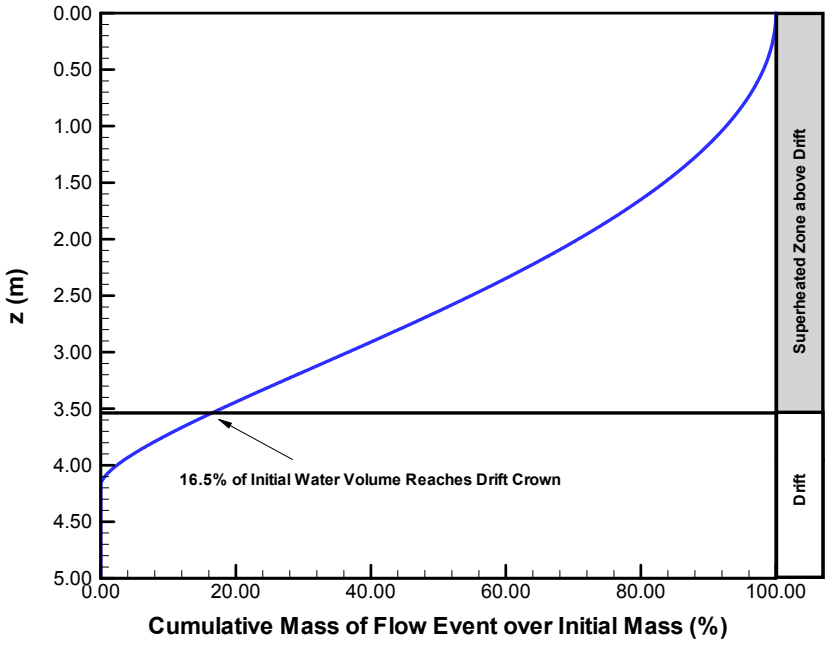


Figure 4. Total water mass breakthrough at location z at 550 years of heating

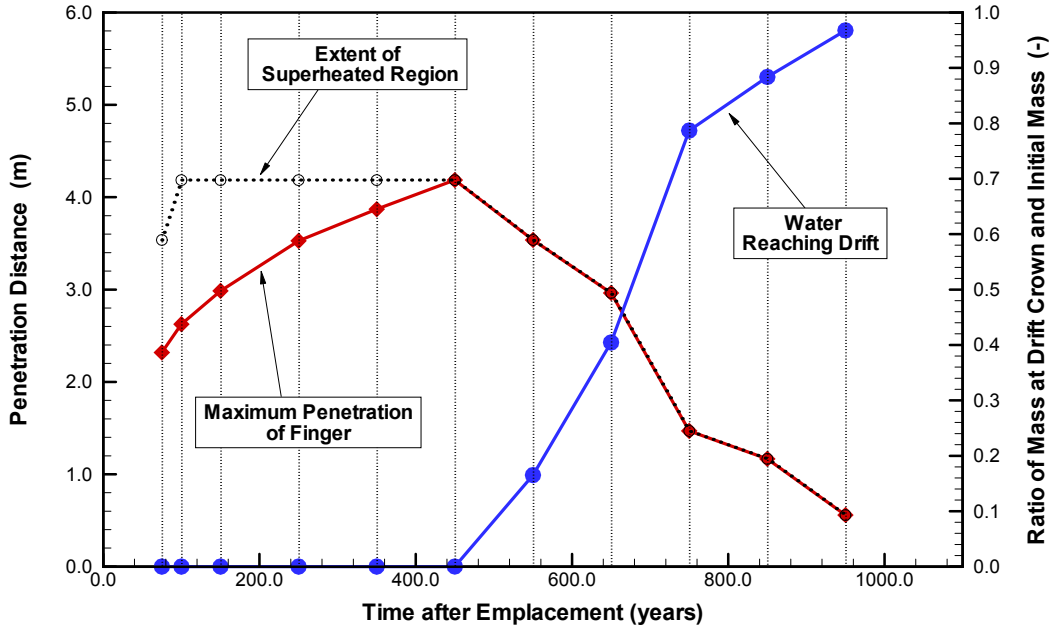


Figure 5. Maximum penetration and percentage of water mass arriving at drift crown, at 11 different time steps after waste emplacement

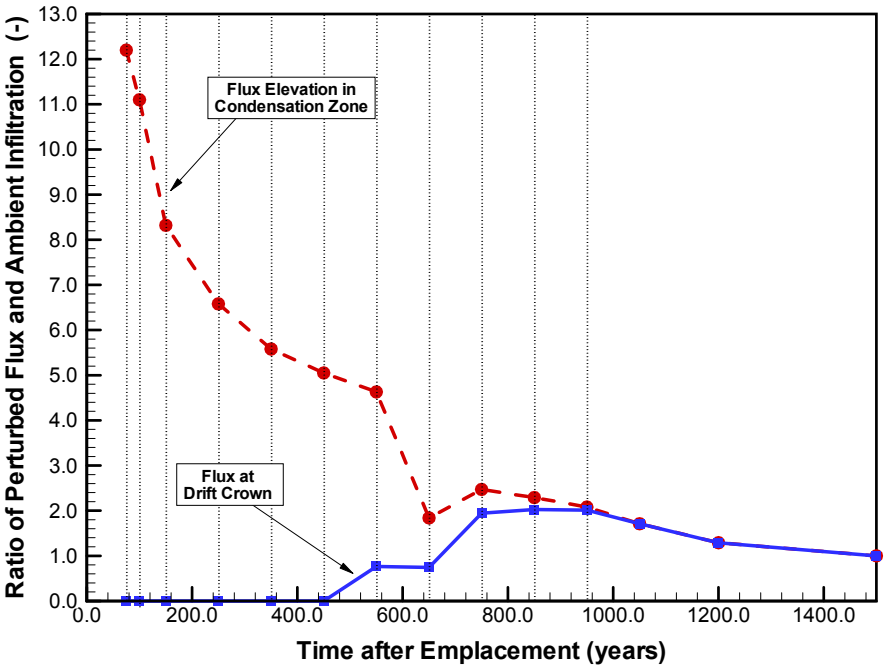


Figure 6. Ratio of thermally perturbed vertical flux and natural infiltration.

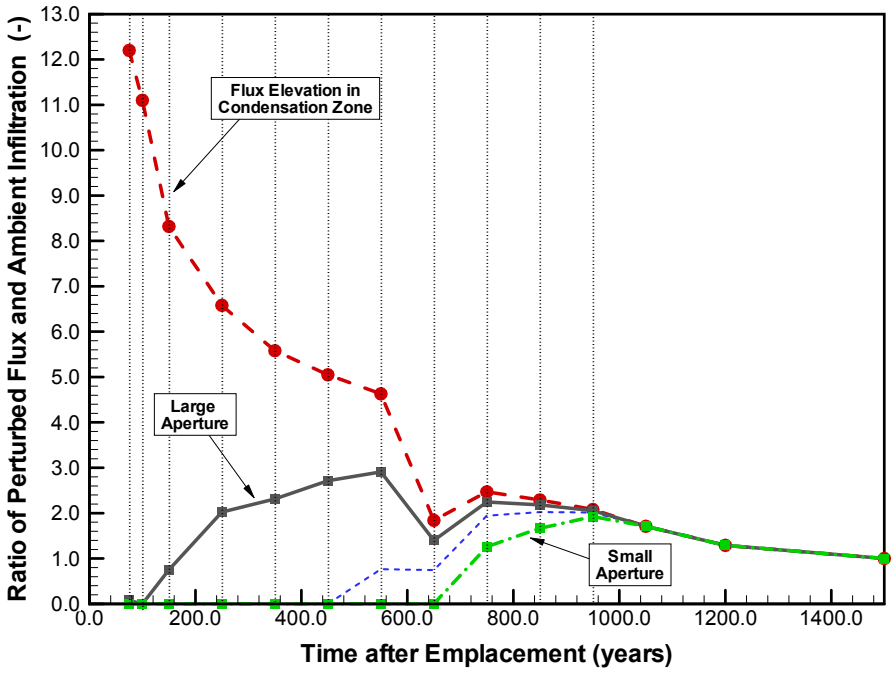


Figure 7. Ratio of thermally perturbed vertical flux and natrual infiltration, showing sensitivity of model results to fracture aperture

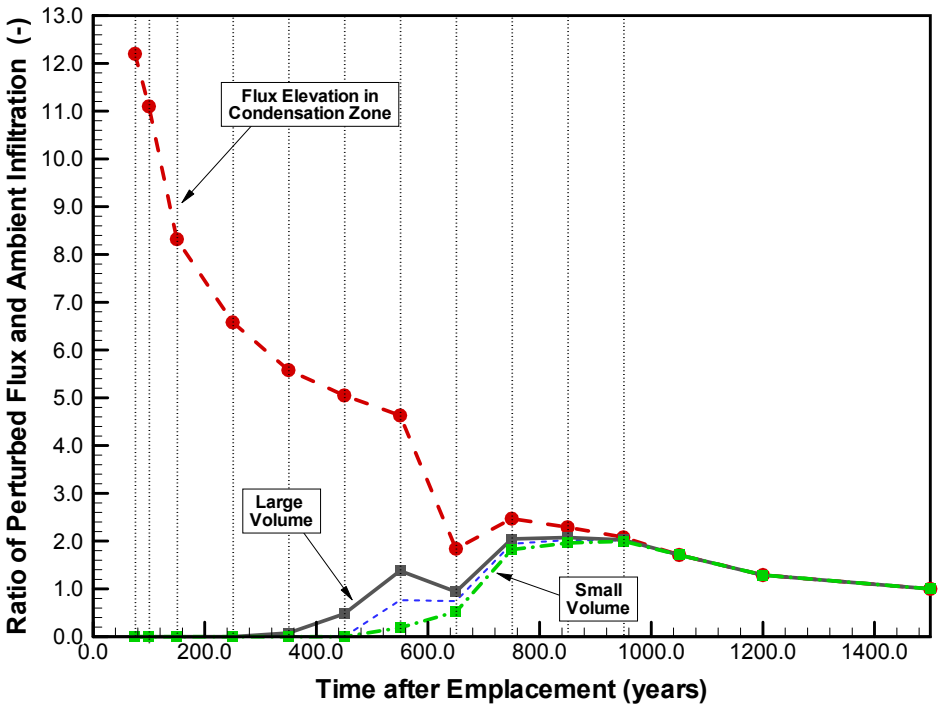


Figure 8. Ratio of thermally perturbed vertical flux and natural infiltration, showing sensitivity of model results to initial water volume